Published in final edited form as:
J Mol Cell Cardiol. 2014 July ; 72: 296–304. doi:10.1016/j.yjmcc.2014.04.005.

Tri-iodo-L-thyronine Promotes the Maturation of Human Cardiomyocytes-Derived from Induced Pluripotent Stem Cells

Xiulan Yang, Ph. D[1,6,7], **Marita Rodriguez, M.S.**[2], **Lil Pabon, Ph. D**[1,6,7], **Karin A Fischer, B. S.**[3], **Hans Reinecke, Ph. D**[1,6,7], **Michael Regnier, Ph.D**[4,6,7], **Nathan J. Sniadecki, Ph. D**[2,4], **Hannele Ruohola-Baker, Ph. D**[3], and **Charles E. Murry, Ph.D, MD**[1,4,5,6,7]

[1]Department of Pathology, University of Washington, Seattle WA 98109

[2]Department of Mechanical Engineering, University of Washington, Seattle WA 98109

[3]Department of Biochemistry, University of Washington, Seattle WA 98109

[4]Department of Bioengineering, University of Washington, Seattle WA 98109

[5]Department of Medicine/Cardiology, University of Washington, Seattle WA 98109

[6]Center for Cardiovascular Biology, University of Washington, Seattle WA 98109

[7]Institute for Stem Cell and Regenerative Medicine, University of Washington, Seattle WA 98109

Abstract

Background—Cardiomyocytes derived from human induced pluripotent stem cells (hiPSC-CMs) have great potential as a cell source for therapeutic applications such as regenerative medicine, disease modeling, drug screening, and toxicity testing. This potential is limited, however, by the immature state of the cardiomyocytes acquired using current protocols. Tri-iodo-L-thyronine (T3) is a growth hormone that is essential for optimal heart growth. In this study, we investigated the effect of T3 on hiPSC-CM maturation.

Methods and Results—A one-week treatment with T3 increased cardiomyocyte size, anisotropy, and sarcomere length. T3 treatment was associated with reduced cell cycle activity, manifest as reduced DNA synthesis and increased expression of the cyclin-dependent kinase inhibitor p21. Contractile force analyses were performed on individual cardiomyocytes using arrays of microposts, revealing an almost two-fold higher force per-beat after T3 treatment and also an enhancement in contractile kinetics. This improvement in force generation was

Correspondence to: Charles E. Murry, MD, PhD, Center for Cardiovascular Biology, Institute for Stem Cell and Regenerative Medicine, University of Washington, 850 Republican St, Brotman Building Rm 453, Seattle, WA 98109, Phone: 206-616-8685 Fax: 206-897-1540, murry@uw.edu.

Disclosure

CEM is co-founder and equity holder in BEAT Biotherapeutics. NJS is co-founder and equity holder in Stasys Medical Corporation.

Supplementary Material

Supplementary material available online at JMCC website.

accompanied by an increase in rates of calcium release and reuptake, along with a significant increase in sarcoendoplasmic reticulum ATPase expression. Finally, although mitochondrial genomes were not numerically increased, extracellular flux analysis showed a significant increase in maximal mitochondrial respiratory capacity and respiratory reserve capability after T3 treatment.

Conclusions—Using a broad spectrum of morphological, molecular, and functional parameters, we conclude that T3 is a driver for hiPSC-CM maturation. T3 treatment may enhance the utility of hiPSC-CMs for therapy, disease modeling, or drug/toxicity screens.

Keywords

Human induced pluripotent stem cells-derived cardiomyocytes (hiPSC-CMs); Cardiomyocyte maturation; Tri-iodo-L-thyronine; Contractile force; Mitochondria

1. Introduction

With the advent of directed cardiac differentiation, cardiomyocytes can be obtained in large scale from human pluripotent stem cells, such as embryonic stem cells and induced pluripotent stem cells (hESCs and hiPSCs, respectively)[1, 2]. These cardiomyocytes exhibit sarcomeres, calcium transients and spontaneous beating, but they display a low degree of maturation based on all the parameters that have been studied[3]. A general consensus has emerged that maturation protocols must be developed to maximize the therapeutic applications of hiPSC-CMs.

Thyroid hormones (THs) are essential for diverse heart developmental processes. In the rodent perinatal period, for example, T3 regulates isoform switching of titin[4, 5] from fetal to adult type. Titin is involved in the maintenance of sarcomere integrity and elasticity and it shifts from a relatively compliant N2BA isoform to a shorter and stiffer N2B isoform. This isoform switch alters the passive tension generated by maturing cardiomyocytes[6-8]. Also, T3 represses expression of fetal genes in neonatal cardiomyocytes to enhance normal cardiac maturation[5, 9]. In humans, abnormally high TH levels in the fetus can lead to a range of complications, including decreased cardiac output, growth restriction, tachycardia, neuropathologies, and even fetal demise[10-12]. T3 has also been shown to promote the maturation of *in vivo* fetal sheep cardiomyocytes[13], cultured neonatal mouse and rat cardiomyocytes[14], and the cardiomyocytes-derived from murine embryonic stem cells[15]. Notably, upon the birth of a human being, thyroid-stimulating hormone concentrations rise abruptly within 30 to 60 minutes after delivery, resulting in an almost 6-fold increase of serum T3 level[16]. A recent study reported T3 treatment of hiPSC-CMs modulated cardiac gene expression[17]. Based on the evidence from different model systems, we decided to systematically characterize the effect of T3 on the maturation of hiPSC-CMs, using diverse approaches, which included multiple functional endpoints.

In this study, we found that T3-treated hiPSC-CMs exhibited a larger cell size, longer sarcomere length, lower proliferative activity, higher contractile force generation, enhanced calcium handling properties, and increased maximal mitochondrial respiration capacity compared with the untreated control cells. Therefore, these results demonstrate that T3

promotes the maturation of hiPSC-CM and may enhance their utility for therapy, disease modeling, drug screens, and other applications.

2.Methods

2.1. Cell Culture

Undifferentiated human IMR90-induced pluripotent stem cells, originally derived from lung fibroblasts[18] (James A. Thomson, University of Wisconsin-Madison), were expanded using mouse embryonic fibroblast-conditioned medium supplemented with 5 ng/ml basic fibroblast growth factor. Cardiomyocytes were obtained using a protocol based on our previously reported directed differentiation method that involves the serial application of activin A and bone morphogenetic protein-4 (BMP4) under serum-free, monolayer culture conditions. The cultures were also supplemented with the Wnt agonist CHIR 99021 in the early stages of differentiation followed by the Wnt antagonist Xav 939. After 20 days of *in vitro* differentiation, the cells were dispersed using 0.05% trypsin-EDTA and replated. Cultures were fed every other day thereafter with serum-free RPMI-B27 plus L-glutamine. Only cell preparations containing >80% cardiac troponin T-positive cardiomyocytes (by flow cytometry) were used for the current investigation. After 20 days of differentiation, the cells were treated with 20 ng/ml T3 for one week, and media were changed every other day. For cell cycle analysis, cells were treated with 10 μM BrdU overnight before fixation.

2.2. Immunocytochemistry

Cells were fixed in 4% paraformaldehyde for 10 min followed by PBS wash. The fixed cells were blocked with 1.5% normal goat serum for 1 hour at room temperature and incubated overnight at 4°C with primary antibodies. Antibodies used included mouse anti-alpha-actinin (Sigma) and mouse anti-BrdU (Roche). The samples were rinsed with PBS and incubated with a secondary antibody. Samples subjected to F-actin staining were incubated with TRITC-labeled phalloidin (Sigma) for 5 min at room temperature. For double immunostaining samples were stained first for alpha-actinin staining, after which cells were incubated with 1.5N HCl at 37°C for 15 min, rinsed briefly in distilled water, and washed with 0.1 M Borax buffer, and incubated with BrdU primary antibody overnight at 4°C. BrdU staining was then enhanced using tyramide signal amplification method (Invitrogen).

2.3. Imaging and morphological analysis

Fluorescent images were acquired using a Zeiss AxioCam mounted on a Zeiss AxioObserver microscope, and confocal images were processed and quantified using NIS Elements. Each cell was analyzed for cell size and circularity index. For sarcomere length, we selected myofibrils with at least ten continuous, well-recognized α-actinin+ bands and divided the length value by the number of sarcomeres.

2.4. Quantitative PCR

Total RNA was isolated using the Qiagen RNeasy kit, and mRNA was reverse transcribed using the Superscript III first strand cDNA synthesis kit (Invitrogen). All primers were purchased from Real Time Primers, and qPCR was performed using SYBR green chemistry and an ABI 7900HT instrument. Samples were normalized using hypoxanthine-guanine

phosphoribosylthransferase (HPRT) as a housekeeping gene. The sequences of the primers are listed below. The forward primer sequence for β-MHC: GGGCAACAGGAAAGTTGGC, reverse primer: ACGGTGGTCTCTCCTTGGG; Forward primer sequence for SERCA2a: forward TTTCCTACAGTGTAAAGAGGACAACC, reverse primer sequence for SERCA2a: TTCCAGGTAGTTGCGGGCCACAAA; Forward primer sequence for α-MHC: CAAGTTGGAAGACGAGTGCT, Reverse primer sequence for α-MHC: ATGGGCCTCTTGTAGAGCTT; Forward primer sequence for p21: TCAGAGGAGGTGAGAGAGCG, reverse primer sequence for p21: ACATGGCGCCTGCCG. Primers to detect titin isoform switch is from[19]. Forward primer sequence for total titin: GTAAAAAGAGCTGCCCCAGTGA, Reverse primer sequence for total titin: GCTAGGTGGCCCAGTGCTACT; Forward primer sequence for titin N2BA isoform: CAGCAGAACTCAGAATCGA, reverse primer sequence for titin N2BA isoform: ATCAAAGGACACTTCACACTC; Forward primer sequence for titin N2B isoform: CCAATGAGTATGGCAGTGTCA, reverse primer sequence for titin N2B isoform: TACGTTCCGGAAGTAATTTGC. Forward primer sequence for HPRT: TGACACTGGCAAAACAATGCA, reverse primer sequence for HPRT: GGTCCTTTTCACCAGCAAGCT. Mitochondrial DNA (mtDNA) to nuclear DNA (nDNA) ratio was estimated by qPCR. For this purpose, a mtDNA fragment within the NADH dehydrogenase 1 (ND1) gene and a region of the nuclear DNA-encoded lipoprotein lipase gene (LPL) were amplified. The primer sequences for ND1 and LPL were adapted from[20]. The forward primer sequence for ND1: CCCTAAAACCCGCCACATCT, and the reverse primer was GAGCGATGGTGAGAGCTAAGGT. The LPL forward primer used was CGAGTCGTCTTTCTCCTGATGAT and reverse primer was TTCTGGATTCCAATGCTTCGA. Total DNA was extracted using phenol-chloroform extraction method.

2.5 Western Blotting

Total protein was acquired from control cardiomyocytes or cardiomyocytes after one week of T3 treatment and subjected to SDS-PAGE. The lanes were loaded with equal amount of protein and were checked by Ponceau S staining. After blocking with milk, the membranes were incubated with anti-p21 mouse monoclonal antibody (Cell Signaling Technology) or anti-GAPDH mouse monoclonal antibody (Abcam) overnight while shaking at 4°C. After incubation with anti-mouse horseradish peroxidase-coupled secondary antibody (Santa Cruz Biotechnology), bands were visualized with SuperSignal West Femto Trial Kit (Thermo Scientific) and quantified using the Quantity One software from BioRad.

2.6. Contractile force measurement

Arrays of silicone microposts were fabricated by casting polydimethylsiloxane (PDMS) from a silicon wafer with patterned SU8 features as previously described[21]. The microposts used in this study were 6.45 μm in height and 2.3 m in diameter, and the center-to-center spacing between adjacent microposts was 6 μm. The stiffness of each micropost, which is based upon the dimensions of the microposts and the material properties of PDMS, was 38.4 nN/μm. To enable cell attachment, the tips of these microposts were stamped with 50 μg/ml of mouse laminin (Life Technologies) via microcontact printing, while the remaining surfaces of the micropost array were fluorescently stained with BSA conjugates with Alexa

Fluor 594 and blocked with 0.2% Pluronic F-127 (in PBS)[22]. Twenty days following differentiation, iPS-derived cardiomyocytes were seeded onto the arrays at a density of 250,000/cm^2. One week after T3 treatment, individual cardiomyocyte twitch forces were recorded under phase light using high-speed video microscopy as previously described[23]. Only the contractile forces of single cardiomyocytes (no junctions with adjacent cells) with obvious beating activity were assessed. The experiments were performed in a live cell chamber at 37°C with 15 mM HEPES-containing medium. Post deflections were optically measured at 100-150 frames/sec using phase contrast microscopy on a Nikon Ti-E upright microscope with a 60× water immersion objective. A custom-written MATLAB code was used to compare each time frame of the video to a reference fluorescent image of the base plane of the posts. Twitch forces were subsequently calculated by multiplying the deflection of the posts by the bending stiffness of the microposts:

$$F = k\delta \quad (1)$$

where F is the force at a single micropost, k is the post's bending stiffness (38.4 nN/ m), and δ is the horizontal distance between the centroid of the post's tip and the centroid of the post's base. The total twitch force was then determined by adding together the forces measured at each post beneath the individual cardiomyocytes.

2.7. Calcium imaging

Intracellular calcium content was measured using the ratiometric indicator dye fura2-AM as described previously[24]. For this assay, cardiomyocytes were replated onto fibronectin-coated glass slides, after which the cardiomyocytes were subsequently treated for one week. On the experimental day, cells were incubated in 1 μM fura2-AM dye for 20 min at 37°C and washed with P BS. Stimulated calcium transients (0.5 Hz) were then monitored with the Ionoptix Stepper Switch system coupled to a Nikon inverted fluorescence microscope. The fluorescence signal was acquired using a 40× Olympus objective and passed through a 510-nm filter, and the signal was quantified using a photomultiplier tube. The experiments were done at 37°C with culturing medium containing 15 mM HEPES.

2.8. Mitochondria functional assay

The Seahorse XF96 extracellular flux analyzer was used to assess mitochondria function. The plates were pre-treated with 0.1% Gelatin. At around 20 days after differentiation, the cardiomyocytes were seeded onto the plates with a density of 30,000 per XF96 well (2,500/mm^2). The cells were treated with 20 ng/ml T3 for one week in the Seahorse plates before the assay. Culture medium was exchanged for base media (unbuffered DMEM, Sigma D5030, supplemented with 2 mM glutamine) 1 hour before the assay and for the duration of the measurement. Substrates and selective inhibitors were injected during the measurements to achieve final concentrations of glucose at 25 mM, oligomycin (2.5 μM), FCCP (1 μM), rotenone (2.5 μM), and antimycin A (2.5 μM). The oxygen consumption rate (OCR) values were further normalized to the number of cells present in each well, quantified by the Hoechst staining (Hoechst 33342; Sigma-Aldrich) as measured using fluorescence at 355 nm excitation and 460 nm emission. The baseline OCR was defined as the average values measured from time point 1 to 5 (0–15 min) during the experiments. Maximal OCR

was the OCR difference between uncoupler FCCP and (rotenone + antimycin A), with respiratory reserve capacity being the difference between FCCP and baseline OCR values. Non-mitochondrial OCR was the OCR value after rotenone and antimycin A treatment. Due to variations in the absolute magnitude of OCR measurements in different experiments, the relative T3 treated/untreated control levels were used to compare and summarize independent biological replicates (n = 6).

2.9. Statistics

Data are expressed as mean ± SEM. Differences were compared by ANOVA with Student-Newman-Keuls post hoc testing. $P < 0.05$ was considered significantly different.

3. Results

3.1. T3 treatment leads to hiPSC-CM morphological and molecular changes

Since cardiac maturation results in an increase in cell size and anisotropy, we first characterized the effect of T3 on these parameters. Immunocytochemical co-staining of F-actin and α-actinin (Z-disk protein) was performed to assess morphology. It is worth mentioning that, for all the assays in the current investigation, only differentiation runs with over 80% cardiomyocytes were used (assessed by flow cytometry for $cTnT^+$ cells). Immunocytochemical analyses with α-actinin as a cardiomyocyte marker and Hoechst 33342 for a nuclear counterstain showed that T3 treatment does not lead to a change in cardiomyocyte percentage. Untreated hiPSC-CMs were small and round to polygonal in shape, consistent with previous reports[25]. We observed a significant increase in cell size (cell area) in T3-treated cells compared with control cells (604 ± 28 μm^2 vs. 991 ± 58 μm^2, $P<0.001$), shown in Fig. 1C. To determine cardiomyocyte shape, we assessed the "circularity index" ($Circularity = 4\pi \cdot Area / Perimeter^2$)[26]. Under this assessment, "0" represents a theoretical minimum for perfect rod-shaped cells (actually, a line with no area), with "1" for cells that are perfectly circular. T3-treatment resulted in a decreased circularity index (0.66 ± 0.03 vs 0.54 ± 0.02 P=0.004) (Fig. 1D), indicating that the hiPSC-CMs exhibited a more mature morphology. Additional analyses showed that the sarcomere length (measured by the distance between Z-disks) increased from 1.67 ± 0.02 μm in untreated controls to 1.73 ± 0.01 μm (P=0.006) in T3-treated cells (Fig. 1E).

We also compared the expression of various cardiac genes in control and T3-treated cells by quantitative RT-PCR. Consistent with previous reports of T3's effects on cardiac gene expression[5, 17], we observed α-MHC up-regulation (7.3 ± 1.9-fold vs. control), β-MHC down-regulation (0.5 ± 0.2-fold vs. control), and an increase of sarcoendoplasmic reticulum ATPase (SERCA2a) expression (3.9 ± 0.9-fold vs. control) (Fig. 1F). We also examined whether a titin isoform switch from N2BA to N2B could be detected in our culture system by Q-RT-PCR assay. Both N2BA and N2B isoforms were expressed with N2BA being the dominant one. One week of T3 treatment did not change the expression level of either isoform (data not shown). In the cardiomyocytes derived from human Rockefeller University Embryonic Stem Cell Line 2, T3 treatment induced similar cardiac gene expression patterns. We observed a 4.35-fold and a 10.78-fold upregulation of α-MHC after 2.5 and 14 days treatment, respectively, whereas the expression of β-MHC decreased 0.73-

fold and 0.48-fold. An increase of 1.88-fold (2.5 days) and 3.93-fold (14 days) was detected for SERCA2a.

3.2. Effects of T3 on cardiomyocyte cell cycle activity

During development, the proliferative capacity of maturating cardiomyocytes decreases, leading to an eventual exit of the cell cycle[1]. We assessed cell cycle activity by pulsing the cells overnight with BrdU, followed by double-staining for α-actinin and BrdU (Fig. 2A and 2B). The total number of hiPSC-CM nuclei, as well as the BrdU-positive cardiomyocyte nuclei, were counted in three separate experiments. In the control groups, about 8.0% of cardiomyocyte nuclei were BrdU-positive, while after T3 treatment, the number declined to around 4.2% (Fig. 2C). Consistent with the changes in cell cycle activity, both mRNA levels and protein levels of the cell cycle inhibitor p21 were increased after T3 treatment (Fig. 2D and 2F). A representative p21 immunoblot is shown in Fig. 2E. Thus, supporting the role of T3 in the regulation of hiPSC-CMs maturation, our study showed lower proliferation rates in the T3 treated cultures as compared to those of control cells. Since adult human cardiomyocytes exhibit about 25% binucleation, we also analyzed whether T3 treatment influenced this maturation parameter. No differences were found in the percentage of binucleated cells between groups, with both around 12%.

3.3. T3-treatment improves contractile force generation and enhances contractile kinetics

As mentioned above, sarcomere length increased after T3 treatment. Since an increase in sarcomere length within the range of 1.6 to 2.3 μm in cardiac muscle typically leads to an increase in force production, we hypothesized that T3 treatment leads to greater contractile force generation. To characterize force production on a per-cell basis we used micropost arrays[27]. For this approach, individual cardiomyocytes were allowed to adhere to elastomeric microposts with uniform heights, diameters, and spacing between the microposts (Fig 3A). As the cardiomyocytes contract, the deflections of the posts underneath a cell were recorded. By applying beam theory, the forces produced at each adhesion of a cardiomyocyte can be calculated by multiplying the deflection of each post by its spring constant (eq. 1). The magnitude of the forces vectors can be summed to obtain the total force produced by a cell at each time point. Fig. 3B shows representative traces of the total force generated by individual cardiomyocytes from the control and T3-treated groups. Control hiPSC-CMs exhibited a twitch force of 7.5 ± 0.4 nN/cell (Fig 3C). T3-treated hiPSC-CMs exhibited a significantly higher twitch force of 12.3 ± 0.7 nN/cell ($P<0.001$). Contractile time analysis revealed that T3-treated hiPSC-CMs displayed shorter time to peak contraction (0.15 ± 0.01 sec versus 0.25 ± 0.02 sec in control cells, as shown in Fig. 3D). T3 also significantly decreased the time to 90% relaxation (Fig. 3E) and total twitch time (Fig. 3F). Two representative movies for control and T3-treated cardiomyocytes can be found in the supplemental material. These data demonstrate that T3-treatment not only results in morphological and molecular changes indicative of maturation, but that functionally relevant parameters such as contraction are also positively-regulated.

3.4. T3-treated cardiomyocytes exhibit faster calcium transient kinetics

To further investigate the mechanism underlying changes in cardiomyocyte performance, we compared the calcium transient characteristics of untreated and T3-treated hiPSC-CMs using

the intracellular calcium ratiometric dye fura-2 AM. A representative trace is shown in Fig. 4A. While the peak transient amplitude remained unchanged after treatment (0.24 ± 0.03 vs 0.20 ± 0.02 F/F0, P=0.23) (Fig. 4B), the maximal upstroke and decay velocities were significantly higher in T3-treated cells (Fig. 4C and 4D). More specifically, Vmax upstroke was faster (2.99 ± 0.64 vs. 7.43 ± 1.43 F/F0/sec, P= 0.004) and time to 90% peak $[Ca^{2+}]_i$ was significantly shorter (0.52 ± 0.08 vs. 0.25 ± 0.06 sec, P=0.029) after T3 treatment. A faster Ca^{2+}-transient decay rate (0.39 ± 0.03 vs 0.55 ± 0.07 F/F0/sec, P=0.028), and significant shorter time to 50% decay (0.51 ± 0.05 vs 0.33 ± 0.04 sec, P=0.0141) was observed after T3 treatment.

3.5. Effect of T3-treatment on mitochondria

Mitochondria are essential cellular organelles for cardiac cells, which generate enough ATP to allow contraction. During development, mitochondria evolve both morphologically and functionally. The ratio of mtDNA to nDNA genomes was around 600 for both control and T3 treated cardiomyocytes with no significant differences. Electron microscope images were taken and mitochondria volume fraction was evaluated by point counting. No difference was found in the mitochondrial volume fraction, which averaged ~7% in both groups (supplemental data). To characterize mitochondrial function, a Seahorse XF96 extracellular flux analyzer was used. We found that hiPSC-CMs have sufficiently active glycolysis to support metabolism while mitochondrial function is manipulated. As a result, we could measure all of the major aspects of mitochondrial coupling and respiratory control. Basal respiration, maximum respiration rate, spare respiratory capacity, and non-mitochondrial respiration can be determined by the sequential additions of the ATP synthase inhibitor oligomycin, a protonophoric uncoupler FCCP, and electron transport inhibitors, rotenone and antimycin A. Fig. 5A shows representative traces of both control and T3-treated cells.

Basal respiration is usually controlled strongly by ATP turnover and partly by substrate oxidation and proton leak. After treatment with T3, basal respiration increases significantly (Fig. 5B), which correlates with the enhanced contractile force generation in these cells. Maximum respiration rate was significantly increased after T3-treatment. Non-mitochondrial respiration is mediated by various enzymes in the cell membrane and cytoplasm, which control detoxification and oxidation. In this experiment, for both control and T3-treated cells, non-mitochondrial OCR was 20-30% of total OCR and there is a significant increase of non-mitochondrial OCR after T3 treatment.

4. Discussion

Due to the difficulty of acquiring human cardiomyocytes, the production of large quantities of hiPSC-CMs offers an attractive source for heart regeneration, disease modeling, drug screening, and toxicity testing. These hiPSC-CMs, however, do not recapitulate the major characteristics (structure, contractile performance, electrophysiology, and metabolism) of adult cardiomyocytes, rather, they exhibit an immature phenotype more closely resembling fetal cells[3]. These immature characteristics, have limited the use of hiPSC-CMs as a substitute for adult human cardiomyocytes for both *in vivo* and *in vitro* applications. In this particular study, we investigated the effect of T3 on hiPSC-CM maturation.

Control hiPSC-CMs exhibited immature morphological and functional characteristics, in agreement with previous reports[25]. Here we showed that after T3 treatment, the cardiomyocytes grew in size and became more anisotropic. The importance of cell size is reflected in the fact that it influences impulse propagation, maximal rate of action potential depolarization and total contractile force[28]. It is worth mentioning that T3 has been associated with both physiological and pathological hypertrophy, depending on the clinical context (e.g. postnatal growth vs. hyperthyroidism). However, the hypertrophy observed in this study appears to be physiological, because it is accompanied by enhanced calcium dynamics, enhanced mitochondrial respiratory capacity, and increased contractile force. For detailed discussions of physiological versus pathological hypertrophy, interested readers are referred to reviews by Molkentin's group[29,30]. Cardiomyocyte shape also has important functional implications including the facilitation of excitation-contraction coupling[3]. T3 treatment led to a more elongated cell shape, possessing a morphological property one step closer to adult cardiomyocytes.

T3 treatment increased the spontaneous contractile force generation from ~7.5 nN/cell to ~12.3 nN/cell (Fig. 3). Using different approaches and substrates of varying stiffness, individual hPSC-CM forces have been measured in the range of 0.1 nN to almost 100 nN[31-35]. Typically, cardiomyocytes generate more force on stiffer substrates. For this current study, we used arrays of microposts to measure the contractile force produced by individual hiPS-derived cardiomyocytes. A recent study[35] employed similar microfabricated platforms to measure the contractile force of human embryonic stem cell-derived cardiomyocytes. They recorded forces between 50 and 100 nN/cell for cells seeded onto 0.01 N/m (10 nN/μm) microposts. These values are almost ten times larger than the results that we found for our control group. A number of different variables could have led to this discrepancy, including different stem cell lines, differentiation and culture conditions, different device calibrations, etc. Additionally, it is worth mentioning that without cell staining in the study by Taylor et al, it may be hard to differentiate whether the forces measured were generated by individual cardiomyocytes or by clusters of cardiomyocytes. Furthermore, since the microposts used in their study were about 10 times larger than the ones we used, it is possible that there were more integrin molecules engaged (and thus, focal adhesion complexes) between the cells and posts in their studies. The spacing may also have led to the elongation and myofibrillar alignment of these cells. However, without sarcomeric visualization, one cannot assess the alignment hypothesis and determine exactly how many cells contributed to the measured force.

Assessment of mitochondrial function showed a significant 1.5-fold increase in maximal respiratory capacity after T3 treatment, which indicates a more mature metabolic state of the cardiomyocytes. Although this could theoretically result from increased mitochondria biogenesis, neither the mtDNA/nDNA ratio nor the mitochondrial volume fraction supports this possibility. Remaining possibilities include: 1) increased respiratory chain protein content, or 2) increased activity of existing respiratory chain proteins. The exact mechanism underlined this effect remains to be explored. Mitochondrial respiratory reserve capacity serves the increased energy demands when cells are subjected to stress, thereby helping maintain cell and organ function, cellular repair, or detoxification of reactive species[36]. T3

treatment led to an increase in respiratory reserve capacity, indicating that the treated cells may perform better under increased energy demands.

Although T3-treated cardiomyocytes were clearly more mature than the control cells, it is important to recognize that the improvement in maturation is by no means complete. T3 receptors have been shown to bind with α-MHC promoter to induce α-MHC and microRNA 208a expression. MicroRNA 208a, in turn, inhibits the expression of β-MHC[37]. This decrease in β-MHC expression is the opposite of what one would expect to see in the case of human cardiomyocyte maturation. This highlights the limitations of using a single factor to induce a complex trait like maturation. Another potential limitation is the duration of treatment. The total maturation time in our study was around one month (~3 weeks from beginning differentiation to beginning the 1-week T3 treatment), whereas human neonatal cardiomyocytes require 6 to 10 years *in vivo* to reach their adult phenotype[38]. Supporting the benefits of time and patience, a report from Lundy and colleagues[25] showed a significant increase in various maturation parameters upon the long-term (~100 day) maintenance of hPSC-CMs in low density cultures. Comparing the results from parameters that were characterized in both the long-term culture and T3 studies, we found that these two maturation approaches resulted in similar increases in calcium handling properties. Morphological changes (size and circularity index), however, were not as pronounced in the T3 cultures as the long-term cultured ones. Contractile performance was assessed using different approaches, thus a direct comparison will be necessary for a meaningful conclusion regarding this parameter. However, it is worth mentioning that compared with the long-term culture, which resulted in a significant increase in sarcomere length from 1.65 ± 0.02 μm to 1.81 ± 0.01 μm, one week T3 treatment increased sarcomere length from 1.67 ± 0.02 μm to 1.73 ± 0.01 μm. Considering that the total time of differentiation and maturation in our assay was around one month, we conclude that T3 treatment is a step forward in the efforts to mature the hiPSC-CMs in a timely manner. Since developing cardiac cells *in vivo* are exposed to the combined effects of diverse cues including extracellular matrix, soluble factors, mechanical signals, substrate stiffness, and electrical fields, it seems likely that a combinatorial approach will lead to even better results.

While our T3-treated hPSC-CMs exhibited a degree of structural and functional maturation compared with control untreated cardiomyocytes, the current study did not focus on the downstream signal transduction. Thyroid hormone signaling is reasonably well understood, and it can involve receptors that bind to T3 and translocate to the nucleus and mediate effects via transcriptional regulation. Lee et al. reported that T3 promotes cardiac differentiation of murine embryonic stem cells via the classical genomic pathway, as evidenced by the fact that a thyroid nuclear receptor antagonist bisphenol A significantly reduced the percentage of T3-induced cardiomyocytes[15]. Actions of thyroid hormone that are not initiated by nuclear receptors are termed non-genomic[39, 40] and the signal may be initiated at the plasma membrane or in the cytoplasm. Plasma membrane-initiated actions begin at a receptor on integrin αvβ3 that activates Extracellular signal-Regulated Kinase 1/2. Also, T3 can activate phosphatidylinositol 3-kinase by a mechanism that may be cytoplasmic in origin or may begin at integrin αvβ3. In addition, T3 effects could be mediated by T3 receptors localized in the mitochondria[41]. The effect of T3 observed in this

study might also result from 3,5-diiodothyronine (T2)[42], which is a metabolite of T3 and could stimulate cellular/mitochondrial respiration by a nuclear-independent pathway.

In summary, we have shown that T3 is a driver for hiPSC-CM maturation. For this purpose, we utilized a series of morphological, molecular, and functional assays to assess the various aspects of hiPSC-CMs maturation. Also, this study provides a proof-of-concept and useful baseline data for future work aimed at elucidating the mechanisms underlying these morphological and functional changes. Finally, this study suggests that a combined intervening approach in addition to T3 is needed to promote further maturation of hiPSC-CMs.

Supplementary Material

Refer to Web version on PubMed Central for supplementary material.

Acknowledgments

We are thankful for the technical assistance from Veronica Muskheli (Department of Pathology, University of Washington) and Chiyen Miller (Department of Pathology, University of Washington School of Medicine) for electron microscope experiments.

Sources of Funding

This work was supported by the National Institute of Health grants R01HL084642, P01HL094374, U01HL100405 (to CEM), and P01GM081619 (to CEM and HR-B). Xiulan Yang is supported by the American Heart Association post-doctoral scholarship 12POST11940060. Marita Rodriguez has a NSF Graduate Research Fellowship 2011126228. NJS has an NSF CAREER award CMMI-0846780.

References

1. Laflamme MA, Murry CE. Heart Regeneration. Nature. 2011; 473:326–335. [PubMed: 21593865]
2. Burridge PW, Keller G, Gold JD, Wu JC. Production of De Novo Cardiomyocytes: Human Pluripotent Stem Cell Differentiation and Direct Reprogramming. Cell Stem Cell. 2012; 10:16–28. [PubMed: 22226352]
3. Yang X, Pabon L, Murry CE. Engineering Adolescence: Maturation of Human Pluripotent Stem Cell-Derived Cardiomyocytes. Circ Res. 2014; 114:511–523. [PubMed: 24481842]
4. Kruger M, Sachse C, Zimmermann WH, Eschenhagen T, Klede S, Linke WA. Thyroid Hormone Regulates Developmental Titin Isoform Transitions Via the Phosphatidylinositol-3-Kinase/ Akt Pathway. Circ Res. 2008; 102:439–447. [PubMed: 18096819]
5. Klein I, Ojamaa K. Thyroid Hormone and the Cardiovascular System. N Engl J Med. 2001; 344:501–509. [PubMed: 11172193]
6. Lahmers S, Wu Y, Call DR, Labeit S, Granzier H. Developmental Control of Titin Isoform Expression and Passive Stiffness in Fetal and Neonatal Myocardium. Circ Res. 2004; 94:505–513. [PubMed: 14707027]
7. Opitz CA, Leake MC, Makarenko I, Benes V, Linke WA. Developmentally Regulated Switching of Titin Size Alters Myofibrillar Stiffness in the Perinatal Heart. Circ Res. 2004; 94:967–975. [PubMed: 14988228]
8. Warren CM, Krzesinski PR, Campbell KS, Moss RL, Greaser ML. Titin Isoform Changes in Rat Myocardium During Development. Mech Dev. 2004; 121:1301–1312. [PubMed: 15454261]
9. Dillmann WH. Cellular Action of Thyroid Hormone on the Heart. Thyroid. 2002; 12:447–452. [PubMed: 12165105]
10. Breall JA, Rudolph AM, Heymann MA. Role of Thyroid Hormone in Postnatal Circulatory and Metabolic Adjustments. J Clin Invest. 1984; 73:1418–1424. [PubMed: 6715545]

11. Fisher DA. Fetal Thyroid Function: Diagnosis and Management of Fetal Thyroid Disorders. Clin Obstet Gynecol. 1997; 40:16–31. [PubMed: 9103947]
12. Macchia PE. Recent Advances in Understanding the Molecular Basis of Primary Congenital Hypothyroidism. Mol Med Today. 2000; 6:36–42. [PubMed: 10637573]
13. Chattergoon NN, Giraud GD, Louey S, Stork P, Fowden AL, Thornburg KL. Thyroid Hormone Drives Fetal Cardiomyocyte Maturation. FASEB J. 2012; 26:397–408. [PubMed: 21974928]
14. Deng XF, Rokosh DG, Simpson PC. Autonomous and Growth Factor-Induced Hypertrophy in Cultured Neonatal Mouse Cardiac Myocytes. Comparison with Rat. Circ Res. 2000; 87:781–788. [PubMed: 11055982]
15. Lee YK, Ng KM, Chan YC, Lai WH, Au KW, Ho CY, Wong LY, Lau CP, Tse HF, Siu CW. Triiodothyronine Promotes Cardiac Differentiation and Maturation of Embryonic Stem Cells Via the Classical Genomic Pathway. Mol Endocrinol. 2010; 24:1728–1736. [PubMed: 20667986]
16. Thorpe-Beeston JG, Nicolaides KH, Felton CV, Butler J, McGregor AM. Maturation of the Secretion of Thyroid Hormone and Thyroid-Stimulating Hormone in the Fetus. N Engl J Med. 1991; 324:532–536. [PubMed: 1899469]
17. Ivashchenko CY, Pipes GC, Lozinskaya IM, Lin Z, Xiaoping X, Needle S, Grygielko ET, Hu E, Toomey JR, Lepore JJ, Willette RN. Human-Induced Pluripotent Stem Cell-Derived Cardiomyocytes Exhibit Temporal Changes in Phenotype. Am J Physiol Heart Circ Physiol. 2013; 305:H913–922. [PubMed: 23832699]
18. Yu J, Vodyanik MA, Smuga-Otto K, Antosiewicz-Bourget J, Frane JL, Tian S, Nie J, Jonsdottir GA, Ruotti V, Stewart R, Slukvin II, Thomson JA. Induced Pluripotent Stem Cell Lines Derived from Human Somatic Cells. Science. 2007; 318:1917–1920. [PubMed: 18029452]
19. Makarenko I, Opitz CA, Leake MC, Neagoe C, Kulke M, Gwathmey JK, del Monte F, Hajjar RJ, Linke WA. Passive Stiffness Changes Caused by Upregulation of Compliant Titin Isoforms in Human Dilated Cardiomyopathy Hearts. Circ Res. 2004; 95:708–716. [PubMed: 15345656]
20. Rao M, Li L, Demello C, Guo D, Jaber BL, Pereira BJ, Balakrishnan VS, Group HS. Mitochondrial DNA Injury and Mortality in Hemodialysis Patients. J Am Soc Nephrol. 2009; 20:189–196. [PubMed: 18684894]
21. Tan JL, Tien J, Pirone DM, Gray DS, Bhadriraju K, Chen CS. Cells Lying on a Bed of Microneedles: An Approach to Isolate Mechanical Force. Proc Natl Acad Sci U S A. 2003; 100:1484–1489. [PubMed: 12552122]
22. Sniadecki, NJ.; Chen, CS. Microfabricated Silicone Elastomeric Post Arrays for Measuring Traction Forces of Adherent Cells. In: Wang, Y.; Discher, DE., editors. Methods in Cell Biology: Cell Mechanics. Elsevier Inc.; San Diego, CA: 2007. p. 313-328.
23. Rodriguez ML, Graham BT, Pabon LM, Han SJ, Murry CE, Sniadecki NJ. Measuring the Contractile Forces of Human Induced Pluripotent Stem Cell-Derived Cardiomyocytes with Arrays of Microposts. J Biomechanical Engineering. 2014
24. Korte FS, Dai J, Buckley K, Feest ER, Adamek N, Geeves MA, Murry CE, Regnier M. Upregulation of Cardiomyocyte Ribonucleotide Reductase Increases Intracellular 2 Deoxy-Atp, Contractility, and Relaxation. J Mol Cell Cardiol. 2011; 51:894–901. [PubMed: 21925507]
25. Lundy SD, Zhu WZ, Regnier M, Laflamme MA. Structural and Functional Maturation of Cardiomyocytes Derived from Human Pluripotent Stem Cells. Stem Cells Dev. 2013; 22:1991–2002. [PubMed: 23461462]
26. Jacot JG, McCulloch AD, Omens JH. Substrate Stiffness Affects the Functional Maturation of Neonatal Rat Ventricular Myocytes. Biophys J. 2008; 95:3479–3487. [PubMed: 18586852]
27. Rodriguez AG, Han SJ, Regnier M, Sniadecki NJ. Substrate Stiffness Increases Twitch Power of Neonatal Cardiomyocytes in Correlation with Changes in Myofibril Structure and Intracellular Calcium. Biophys J. 2011; 101:2455–2464. [PubMed: 22098744]
28. Spach MS, Heidlage JF, Barr RC, Dolber PC. Cell Size and Communication: Role in Structural and Electrical Development and Remodeling of the Heart. Heart Rhythm. 2004; 1:500–515. [PubMed: 15851207]
29. Heineke J, Molkentin JD. Regulation of Cardiac Hypertrophy by Intracellular Signalling Pathways. Nat Rev Mol Cell Biol. 2006; 7:589–600. [PubMed: 16936699]

30. Maillet M, van Berlo JH, Molkentin JD. Molecular Basis of Physiological Heart Growth: Fundamental Concepts and New Players. Nat Rev Mol Cell Biol. 2013; 14:38–48. [PubMed: 23258295]

31. Kita-Matsuo H, Barcova M, Prigozhina N, Salomonis N, Wei K, Jacot JG, Nelson B, Spiering S, Haverslag R, Kim C, Talantova M, Bajpai R, Calzolari D, Terskikh A, McCulloch AD, Price JH, Conklin BR, Chen HS, Mercola M. Lentiviral Vectors and Protocols for Creation of Stable Hesc Lines for Fluorescent Tracking and Drug Resistance Selection of Cardiomyocytes. PLoS One. 2009; 4:e5046. [PubMed: 19352491]

32. Lieu DK, Liu J, Siu CW, McNerney GP, Tse HF, Abu-Khalil A, Huser T, Li RA. Absence of Transverse Tubules Contributes to Non-Uniform Ca(2+) Wavefronts in Mouse and Human Embryonic Stem Cell-Derived Cardiomyocytes. Stem Cells Dev. 2009; 18:1493–1500. [PubMed: 19290776]

33. Wang IN, Wang X, Ge X, Anderson J, Ho M, Ashley E, Liu J, Butte MJ, Yazawa M, Dolmetsch RE, Quertermous T, Yang PC. Apelin Enhances Directed Cardiac Differentiation of Mouse and Human Embryonic Stem Cells. PLoS One. 2012; 7:e38328. [PubMed: 22675543]

34. Sun N, Yazawa M, Liu J, Han L, Sanchez-Freire V, Abilez OJ, Navarrete EG, Hu S, Wang L, Lee A, Pavlovic A, Lin S, Chen R, Hajjar RJ, Snyder MP, Dolmetsch RE, Butte MJ, Ashley EA, Longaker MT, Robbins RC, Wu JC. Patient-Specific Induced Pluripotent Stem Cells as a Model for Familial Dilated Cardiomyopathy. Sci Transl Med. 2012; 4:130ra147.

35. Taylor RE, Kim K, Sun N, Park SJ, Sim JY, Fajardo G, Bernstein D, Wu JC, Pruitt BL. Sacrificial Layer Technique for Axial Force Post Assay of Immature Cardiomyocytes. Biomed Microdevices. 2013; 15:171–181. [PubMed: 23007494]

36. Hill BG, Dranka BP, Zou L, Chatham JC, Darley-Usmar VM. Importance of the Bioenergetic Reserve Capacity in Response to Cardiomyocyte Stress Induced by 4-Hydroxynonenal. Biochem J. 2009; 424:99–107. [PubMed: 19740075]

37. Callis TE, Pandya K, Seok HY, Tang RH, Tatsuguchi M, Huang ZP, Chen JF, Deng Z, Gunn B, Shumate J, Willis MS, Selzman CH, Wang DZ. Microrna-208a Is a Regulator of Cardiac Hypertrophy and Conduction in Mice. J Clin Invest. 2009; 119:2772–2786. [PubMed: 19726871]

38. Peters NS, Severs NJ, Rothery SM, Lincoln C, Yacoub MH, Green CR. Spatiotemporal Relation between Gap Junctions and Fascia Adherens Junctions During Postnatal Development of Human Ventricular Myocardium. Circulation. 1994; 90:713–725. [PubMed: 8044940]

39. Davis PJ, Lin HY, Mousa SA, Luidens MK, Hercbergs AA, Wehling M, Davis FB. Overlapping Nongenomic and Genomic Actions of Thyroid Hormone and Steroids. Steroids. 2011; 76:829–833. [PubMed: 21354437]

40. Cheng SY, Leonard JL, Davis PJ. Molecular Aspects of Thyroid Hormone Actions. Endocr Rev. 2010; 31:139–170. [PubMed: 20051527]

41. Blanchet E, Bertrand C, Annicotte JS, Schlernitzauer A, Pessemesse L, Levin J, Fouret G, Feillet-Coudray C, Bonafos B, Fajas L, Cabello G, Wrutniak-Cabello C, Casas F. Mitochondrial T3 Receptor P43 Regulates Insulin Secretion and Glucose Homeostasis. FASEB J. 2012; 26:40–50. [PubMed: 21914860]

42. Goglia F. Biological Effects of 3,5-Diiodothyronine (T(2)). Biochemistry (Mosc). 2005; 70:164–172. [PubMed: 15807655]

Highlights

1. The effect of T3 on the maturation of human iPSC-cardiomyocytes is investigated.
2. T3 treatment increases cardiomyocyte size, anisotrophy, and sarcomere length.
3. T3 reduces cardiomyocyte cell cycle activity.
4. T3 increases contractile force and calcium release and reuptake rates.
5. T3 results in an increase in mitochondrial respiratory capacity.

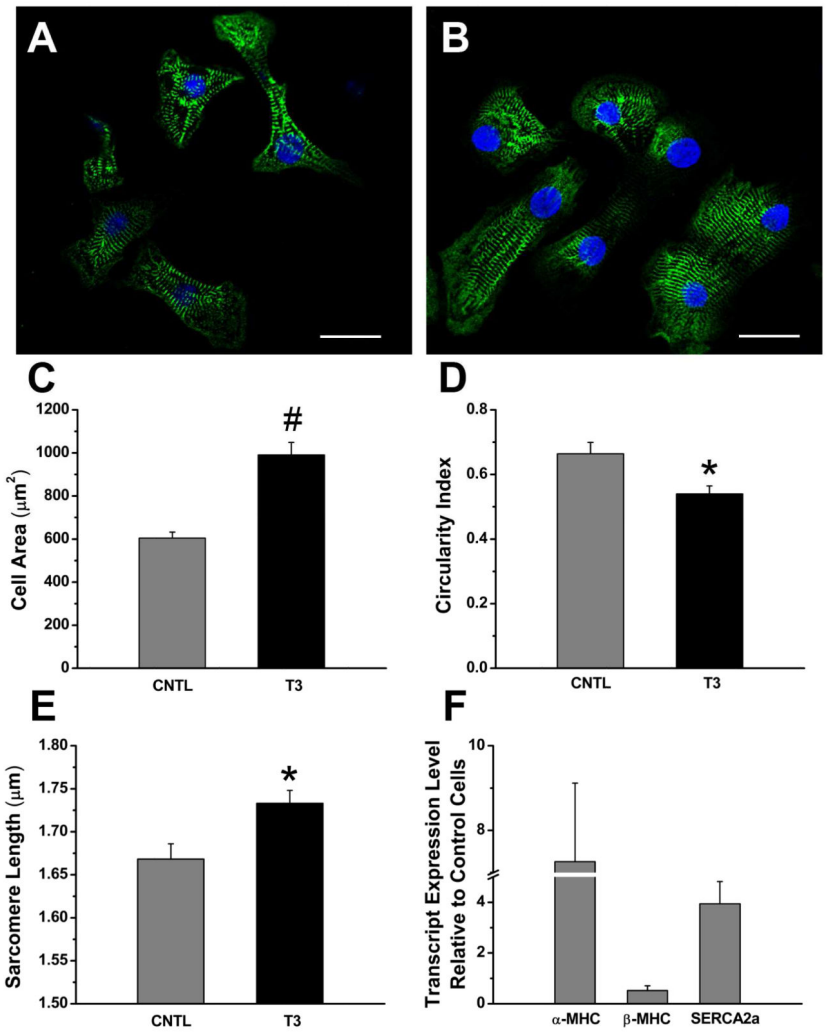

Figure 1.

T3 treatment leads to hiPSC-CM morphological and molecular changes. Representative control (A) and T3-treated (B) cells were stained with α-actinin (green) and Hoechst 33342 (blue). Scale bar: 25 m. Compared to control hiPSC-CMs, T3-treated hiPSC-CMs exhibited significant changes in cell area (C), circularity index (D), and sarcomere length (E). n>100 per condition. # P<0.001, *P<0.05. T3 treatment led to an increase α-MHC, decreased β-MHC, and increased SERCA2a expression level (F). Gene expression is shown normalized first to HPRT mRNA levels and then normalized to untreated control levels.

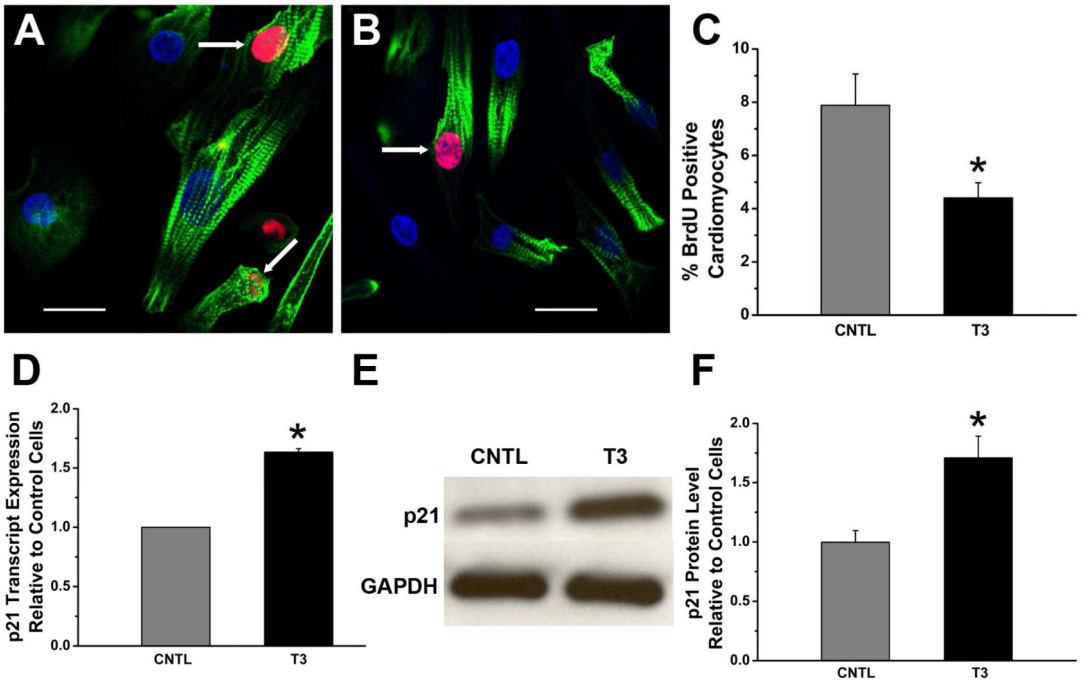

Figure 2.

Effects of T3 on cardiomyocyte cell cycle activity. Cells were treated with 10 μM BrdU overnight and co-stained with α-actinin (green), Hoechst 44432 (blue), and BrdU (red). Double-positive hiPSC-CMs nuclei are magenta (arrows). Representative images for control (A) and after T3 treatment (B) are shown. Scale bar: 25 μm. (C) Quantitative analysis reveals a significant decrease in BrdU-positive percentage of hiPSC-CMs after T3 treatment. * $P<0.05$. $n> 2000$ α-actinin-positive cardiomyocyte nuclei in each group in three separate experiments. (D) Cell cycle inhibitor p21 mRNA transcript expression level compared with control cells (n=3). There is a significant increase in p21 transcript after T3 treatment. (E) Representative immunoblots of p21 and GAPDH in cardiomyocytes from control and T3 groups. (F) Quantitation of western blots demonstrating that p21 protein was significantly elevated in T3-treated cardiomyocytes (n=3). * $P<0.05$ vs. control.

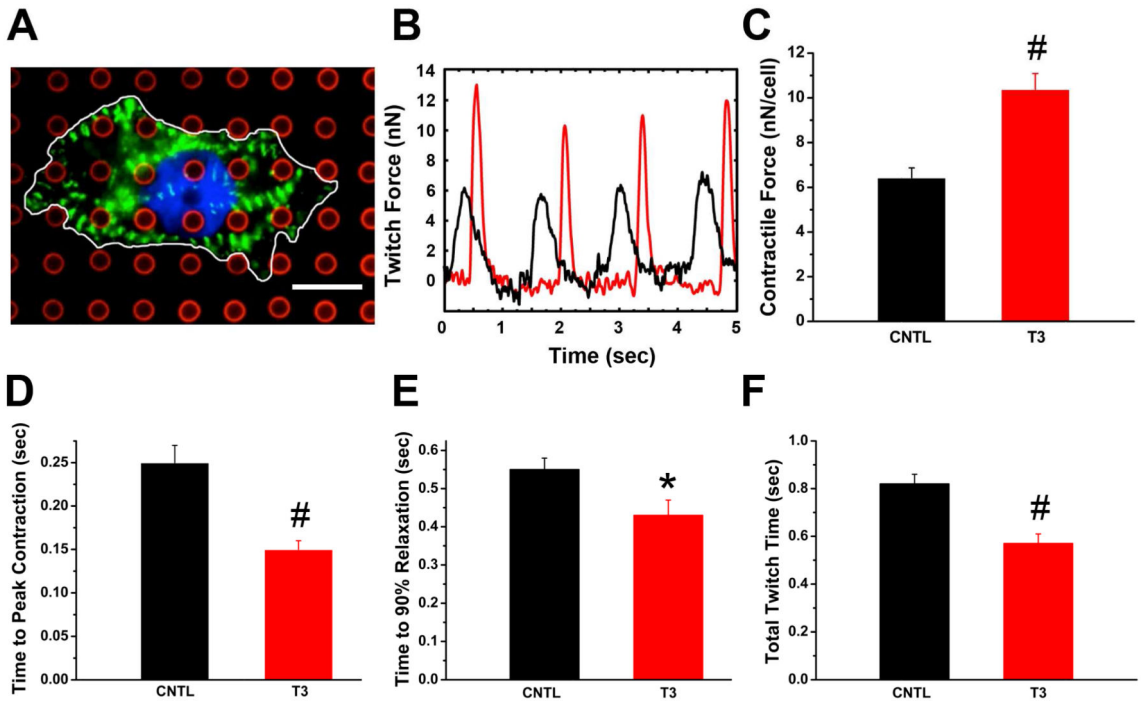

Figure 3.

HiPSC-CMs generate more contractile force after T3 treatment and show enhanced contractile kinetics. (A) representative hiPSC-CM stained for α-actinin (green) and Hoechst 33342 (blue). Microposts that were stained with BSA 594 are shown in red. Scale bar is 10 μm. (B) Representative force traces generated by control and T3-treated hiPSC-CMs. The statistical analysis results are shown in (C). T3 treatment led to significant decrease in time to peak contraction (D), time to 90% relaxation (E), and total twitch time (F). # $P<0.001$ vs. control. N=44 for control hiPSC-CMs and N=66 for T3-treated hiPSC-CMs.

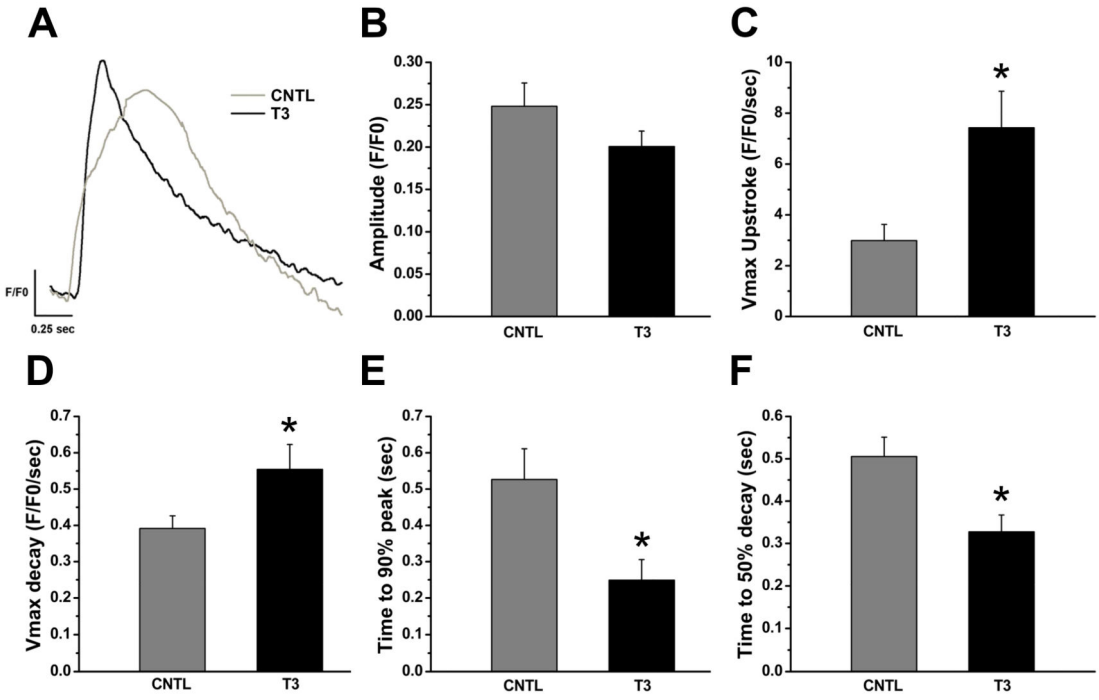

Figure 4.

T3-treated hiPSC-CMs exhibit increased calcium transient kinetics but no change in magnitude. Calcium transients were evaluated by loading the hiPSC-CMs with the intracellular calcium ratiometric indicator fura-2 AM. (A) Representative transients from control and T3-treated hiPSC-CMs. Note the faster upstroke and decay of the Ca^{2+} transient in the T3 cell. (B) The transient amplitude magnitudes were similar, though the calcium kinetics were significantly different in T3-treated hiPSC-CMs, as indicated by increases in maximal upstroke (C) an decay (D) velocities, reduced time to 90% peak $[Ca^{2+}]i$ (E) and (F) reduced time to 50% decay. n=10-15 cells per condition. *P<0.05 vs. control hiPSC-CMs.

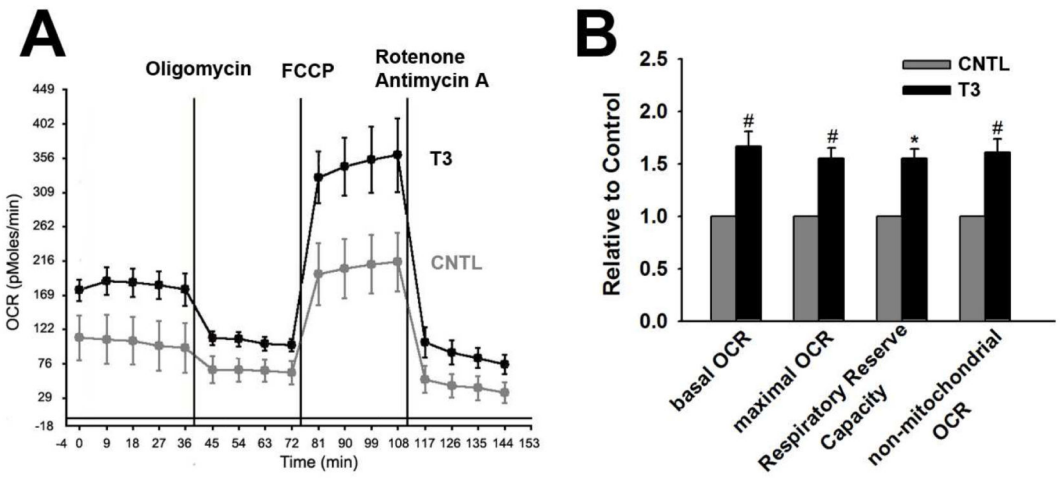

Figure 5.

The effect of T3 on mitochondrial function. Representative traces for control and T3 treated hiPSC-CMs responding to the ATP synthase inhibitor oligomycin, the respiratory uncoupler FCCP, and the respiratory chain blockers rotenone and antimycin A in (A). B shows the statistical analysis of the differences in basal OCR, maximal OCR, respiratory reserve capacity, and non-mitochondrial OCR. * $P<0.05$, # $P<0.001$ vs control hiPSC-CMs. n=6 biological replicates.